

# HYDRATE NUCLEATION MEASUREMENTS USING HIGH PRESSURE DIFFERENTIAL SCANNING CALORIMETRY

Keith C. Hester, Simon R. Davies, Jason W. Lachance,

E. Dendy Sloan, and Carolyn A. Koh\*

Center for Hydrate Research  
Colorado School of Mines  
Golden, CO 80401  
USA

## ABSTRACT

Understanding when hydrates will nucleate has notable importance in the area of flow assurance. Attempts to model hydrate formation in subsea pipelines currently requires an arbitrary assignment of a nucleation subcooling. Previous studies showed that sII hydrate containing a model water-soluble former, tetrahydrofuran, would nucleate over a narrow temperature range of a few degrees with constant cooling. It is desirable to know if gas phase hydrate formers, which are typically more hydrophobic and hence have a very low solubility in water, also exhibit this nucleation behavior.

In this study, differential scanning calorimetry has been applied to determine the hydrate nucleation point for gas phase hydrate formers. Constant cooling ramps and isothermal approaches were combined to explore the probability of hydrate nucleation. In the temperature ramping experiments, methane and xenon were used at various pressures and cooling rates. In both systems, hydrate nucleation occurred over a narrow temperature range (2-3°C). Using methane at lower pressures, ice nucleated before hydrate; whereas at higher pressures, hydrate formed first. A subcooling driving force of around 30°C was necessary for hydrate nucleation from both guest molecules. The cooling rates (0.5-3°C/min) did not show any statistically significant effect on the nucleation temperature for a given pressure.

The isothermal method was used for a methane system with pure water and a water-in-West African crude emulsion. Two isotherms (-5 and -10°C) were used to determine nucleation time. In both systems, the time required for nucleation decreased with increased subcooling.

*Keywords:* Nucleation, DSC, Flow Assurance

## INTRODUCTION

Since 1934 when Hammerschmidt [1] discovered that hydrates were the cause of plugging of natural gas transmission lines, significant research efforts have focused on understanding the conditions that lead to hydrate formation and on the development of chemical hydrate inhibitors. As the oil and gas industry moves into deeper water and corresponding higher pressures from larger liquid heads, the risk of hydrate formation increases. Recent research has concentrated on the rate of formation of a hydrate plug in addition to

continued research on hydrate avoidance. The current state-of-the-art model for hydrate formation CSMHyK [2] relies on two fitted parameters: the formation rate constant and the subcooling at the point of nucleation. Nucleation is the focus of this paper.

Hydrate nucleation is a stochastic event requiring timescales ranging from seconds to thousands of years, as shown by metastable air inclusions in ice cores [3-6]. However, previous studies with a model water-soluble hydrate, tetrahydrofuran (THF) hydrate [7], have shown that with constant

\* Corresponding author: Phone: +1 303 273 3237 Fax +1 303 273 3730 E-mail: ckoh@mines.edu

cooling, a narrow temperature range of a few degrees can cause an increase in the probability of nucleation from almost zero to close to 100%. Before this temperature is reached, it is this very low probability of nucleation that leads to the large variations in nucleation times. While this has been shown for THF hydrate, it is not clear whether this narrow temperature range exists for gas phase hydrate formers, which are more hydrophobic and hence have a very low solubility in water.

In this study, differential scanning calorimetry has been applied to determine the hydrate nucleation point for gas phase hydrate formers. Both constant cooling ramps and isothermal approaches were combined to explore the probability of hydrate nucleation. The effect of cooling rate and subcooling were investigated.

## EXPERIMENTAL METHODOLOGY

### Apparatus

A High Pressure Micro-Differential Scanning Calorimeter ( $\mu$ -DSC) VIIa from Setaram Inc. was used in this study. The  $\mu$ -DSC can be used to measure thermal properties at both atmospheric and pressurized conditions [8]. The pressure is controlled by a gas pressure panel in which a piston can be used to charge the sample with gas at pressures ranging from 1-400 bar. The  $\mu$ -DSC can be used to measure thermal properties of hydrates and ice at these pressures and at temperatures between -45 °C to 120 °C [8].

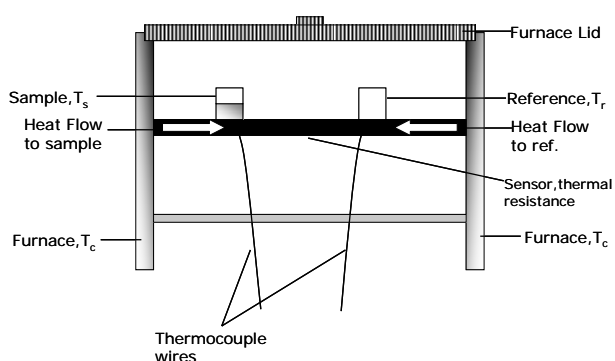


Figure 1 Schematic of DSC furnace showing the process of measurement between the reference and sample cells.

The thermocouples in the calorimetric furnace measure the temperature difference between the

reference and sample cells and record the heat necessary to achieve a zero temperature difference between the cells [9]. Figure 1 shows a schematic of the DSC furnace and a simplified view of the process.

### Procedure/Materials

The main focus of this work was hydrate nucleation using the temperature ramping mode. All temperature ramping experiments were performed by loading around 40 mg of deionized water in a aluminum pressure cell which was then purged multiple times and pressurized to a given pressure with the desired gas: Methane (Airgas, UHP Grade) or xenon (Spectra Gases, UHP Grade). After pressurization, the system was allowed to equilibrate for 3 hours at 40°C. The system was then cooled from 40°C to -40°C between 0.5 to 3°C/min. The temperature was then increased back to 40°C and held for one hour. These ramping cycles were repeated multiple times to determine both the hydrate and ice nucleation temperatures.

The isothermal mode was also used with methane for 175 mg of pure water and for 30 mg of a water-in-oil emulsion - West African crude with a 30% water cut. West African crude is an asphaltenic crude oil with 9.37 wt% asphaltenes and 7.13 wt% resins. The droplet size analysis using DSC was less than 10  $\mu$ m [10]. Following initial pressurization and equilibration at 30°C, the temperature was decreased to either -5 or -10°C. The sample was held at this temperature for approximately six hours. Upon hydrate formation, the sample was heated back up to dissociate the hydrate. The runs were repeated multiple times to observe the time dependence of hydrate nucleation.

### Assignment of phases based on thermograms

The DSC thermogram was used to determine the temperature at which hydrate nucleated. As an example, Figure 2 shows a thermogram for methane + water at 200 bar ramped at 0.5°C/min. Upon cooling, two exothermic responses were measured indicating nucleation and growth of both hydrate and ice phases. These thermal responses are directly proportional to the heat of formation for a given phase change (ice: 334 J/gm-water, sI CH<sub>4</sub> hydrate: 503 J/gm-water) and the mass of the phase formed. However, because of the required

subcooling, both exotherms occurred at temperatures below 0°C. Therefore, further analysis was needed to determine which exotherm corresponded to hydrate and ice nucleation.

Differentiating hydrate exotherms from ice exotherms is relatively straightforward. Hydrate formation from an immiscible guest requires contact between the water and the guest phase, in this case the vapor phase. A thin hydrate film typically forms at the interface. However, water can convert entirely to ice. Hence the ice phase fraction should be much greater than that of the hydrate when formed from a gas phase guest. Due to the similar latent heats of formation, the integrated area of the hydrate exotherm is expected to be much smaller than that for the ice exotherm.

The validity of this hypothesis is verified upon heating. While the nucleation temperature cannot be used to directly distinguish between ice and hydrate below 0°C, endotherms upon heating occur at a given temperature based on phase equilibria. It is then verified that the magnitude of the endotherm is equal to that of the assigned exotherm. As shown in Figure 2, the exotherm and endotherm for the ice phase are approximately equal in area; the same is true for the hydrate phase peaks. This gives added confidence to assigning an exotherm for a given phase.

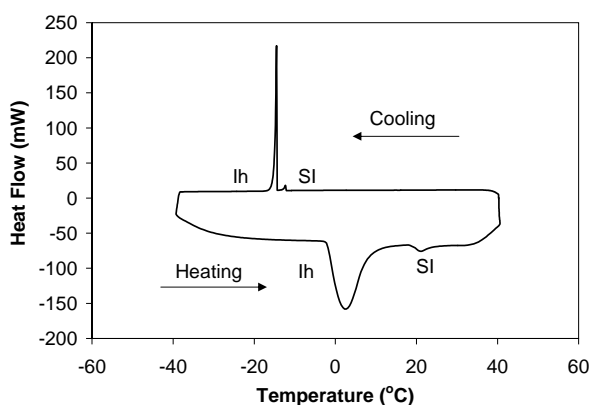


Figure 2 Thermogram for CH<sub>4</sub> + H<sub>2</sub>O at 200 bar with a scanning rate of 0.5°C/min. Formation exotherms are marked for hydrate (SI) and ice (Ih) formation as well as the corresponding melting endotherms when heated.

## RESULTS AND DISCUSSION

### Temperature ramping experiments

#### *Effect of subcooling*

A methane – pure water system was measured to determine the effect of subcooling and cooling rate on hydrate nucleation; both the temperature at which it occurred, and its repeatability. Temperature ramping experiments were performed at 32, 100, 150, and 200 bar with cooling rates of 0.5, 1.5, and 3.0°C/min.

A pressure increase from 32 to 200 bar changed the stability temperature for pure methane hydrate from 2.1 to 18.6°C, which is a significant change in driving force. In these experiments, it was observed that for each pressure, hydrate nucleation always occurred below 0°C. Therefore, ice formation was also possible.

For each pressure, the hydrate nucleated within a 2°C range. An example of this is shown in Figure 3 for methane at 200 bar.

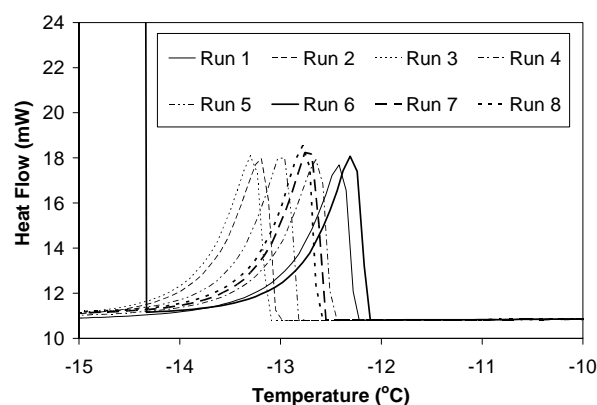


Figure 3 Thermogram of multiple hydrate formation runs using the ramped mode in the DSC with methane + water at 200 bar.

The average nucleation temperature was determined at each pressure and is shown in Figure 4. The error bars show the temperature range in which nucleation occurred. The nucleation temperature for the ice phase is also shown. For the 32 ( $T_{eq} = 2.1^\circ\text{C}$ ) and 100 bar ( $T_{eq} = 12.9^\circ\text{C}$ ) runs, ice always formed before the hydrate. The onset of hydrate nucleation of  $-19.1^\circ\text{C}$  (standard deviation  $0.85^\circ\text{C}$ ) and  $-20.2^\circ\text{C}$  (standard deviation  $0.67^\circ\text{C}$ ) were not statistically different between the 32 and 100 bar runs even with a change of over  $10^\circ\text{C}$  in the driving force. However, the effect of the ice on the tendency for hydrate nucleation is not known. It should be noted that ice formation always occurred between  $-14$  to  $-16^\circ\text{C}$  regardless of pressure and the presence of hydrate.

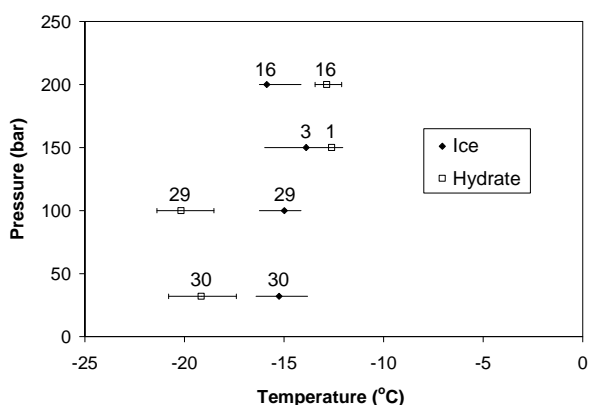


Figure 4 Pressure-temperature plot showing the temperature range for hydrate and ice nucleation at various pressures. Numbers of experiments are shown.

At 150 bar ( $T_{eq} = 16.3^{\circ}\text{C}$ ), ice or hydrate formed first depending on the individual run. From the dissociation endotherms it appeared that in some cases hydrate had nucleated at the same time as ice but the hydrate nucleation peak was obscured by the ice nucleation. In the single experiment where hydrate nucleation was far enough away from ice nucleation to measure, nucleation occurred at  $-12^{\circ}\text{C}$  or a driving force of  $28^{\circ}\text{C}$ . At 200 bar ( $T_{eq} = 18.6^{\circ}\text{C}$ ), hydrate always formed before ice at  $-12.9^{\circ}\text{C}$  (standard deviation  $0.45^{\circ}\text{C}$ ). Interestingly, the change in driving force between 150 and 200 bar roughly coincided with the change in hydrate nucleation temperature.

To further investigate the effect of subcooling on hydrate nucleation, a xenon and pure water system was measured. Xenon is similar in size to methane but it is a much more stable hydrate guest. Experiments were performed in the same manner as the methane system at pressures of 19.5 bar ( $T_{eq}=25.1^{\circ}\text{C}$ ) and 31 bar ( $T_{eq}=29.4^{\circ}\text{C}$ ). Figure 5 shows the fraction of samples that nucleated before a given temperature, for these two pressures. At 19.5 bar, hydrate nucleated at  $-4.9^{\circ}\text{C}$  (standard deviation  $0.7^{\circ}\text{C}$ ) which corresponded to a driving force of  $30^{\circ}\text{C}$ : very similar to the methane system. Hydrate nucleation occurred at  $-2.6^{\circ}\text{C}$  (standard deviation  $0.5^{\circ}\text{C}$ ) for the 31 bar runs. These temperature ramping runs show that similar driving forces are needed to induce nucleation, without the presence of ice, for two different hydrate guests. While this is shown for these experiments, the absolute driving force needed is expected to be very system-dependent.

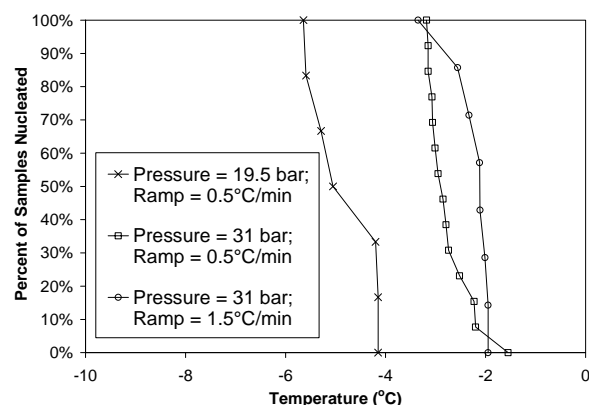


Figure 5 Fraction of samples that nucleated hydrate as a function of pressure and scanning rate for xenon

#### *Effect of cooling rate*

For both systems (methane + water and xenon + water), various cooling rates were employed ( $0.5$ ,  $1.5$ , and  $3.0^{\circ}\text{C}/\text{min}$ ) to determine the effect on the nucleation temperature.

The fraction of samples that nucleated for various cooling rates in a methane system where ice formed first (32 bar) is shown in Figure 6. Figure 7 shows the fraction that nucleated in the case where hydrate formed first (200 bar). In both cases, a  $2.5^{\circ}\text{C}/\text{min}$  change in cooling rate did not have a significant effect on the temperature range in which nucleation occurred. Figure 5 shows two cooling rates for the xenon + water system at 31 bar. As with the methane system, the nucleation point did not change significantly as the cooling rate was increased from  $0.5$  to  $1.5^{\circ}\text{C}/\text{min}$ .

In addition to hydrate nucleation, ice formed during each run with the methane–water system as shown in Figure 4. The onset point of ice nucleation as a function of temperature was measured for various pressures and cooling rates. At 32 and 100 bar, ice formed before hydrate, whereas hydrate formed first at 200 bar. As shown in Figure 8, the pressure, cooling rate, or presence of hydrate had little effect of ice nucleation which occurred between  $-14$  to  $-16^{\circ}\text{C}$  in all cases.

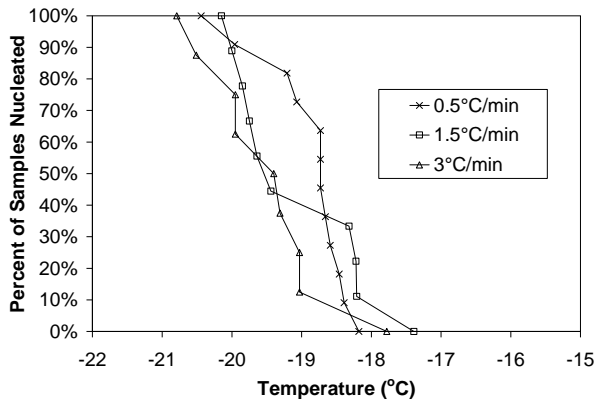


Figure 6 Fraction of samples in which hydrate nucleated as a function of scanning rate for methane-water at 32 bar

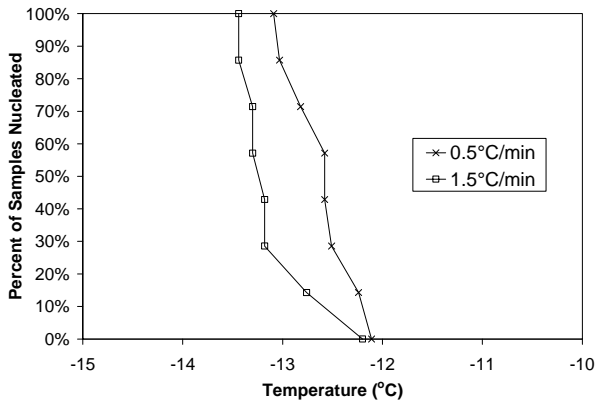


Figure 7 Fraction of samples in which hydrate nucleated as a function of scanning rate for methane-water at 200 bar

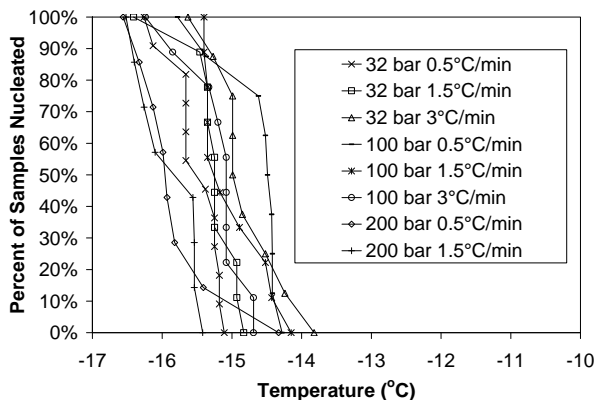


Figure 8 Fraction of samples in which hydrate nucleated as a function of scanning rate for methane-water at pressures of 32, 100 and 200 bar

### Isothermal experiments

The ramped runs have shown that hydrate nucleation is essentially deterministic at a given pressure, within a narrow range of subcooling temperatures. Isothermal runs with methane and pure water showed that the time distribution for hydrate nucleation became narrower at higher subcoolings. Figure 9 shows hydrate nucleation results at 150 bar with 25°C subcooling (-10°C isotherm), 22°C subcooling (-7°C isotherm) and 20°C subcooling (-5°C isotherm).

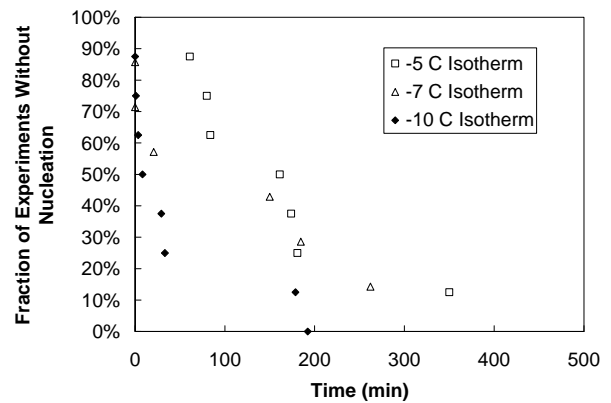


Figure 9 Fraction of samples in which hydrate nucleated at a -5, -7 and -10°C isotherm for methane hydrate at 150 bar

At 25°C subcooling (-10°C isotherm), hydrate nucleation occurred in a narrower time range, from 0-200 minutes than the 20°C (-5°C isotherm) experiments. Most of the runs nucleated within 30 minutes at -10°C. At a subcooling of 20°C (-5°C isotherm) the hydrate nucleation occurred over a wider time range, from 0-1200 minutes.

The -10°C isothermal experiment was also performed (Figure 10) with an emulsified system of water-in-West African crude (WAC) with 30 wt% water cut.

Figure 10 shows that most of the experiments nucleated within 20 minutes. The overall time frame in the emulsified system increased slightly (0-250 min.) compared to the pure system (0-200 min.). The results confirm that at higher subcooling, the rate of hydrate nucleation increases.

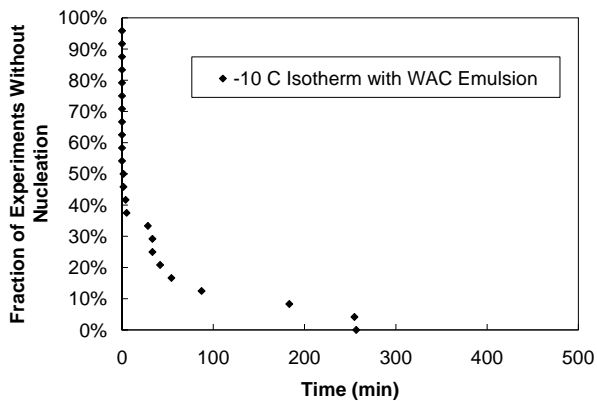


Figure 10 Fraction of samples in which hydrate nucleated in a water-in-West African crude oil emulsion at -10°C isotherm with methane at 150 bar

## CONCLUSIONS

While hydrate nucleation is a stochastic process, the probability of nucleation increases greatly in a narrow band of subcooling of a few degrees, from almost zero to close to 100%. The subcooling needed for this increased nucleation probability was shown for both methane and xenon. The cooling rate did not have a significant effect on nucleation temperature. The time distribution for hydrate nucleation became narrower in isothermal experiments at higher subcoolings. Ice nucleation occurred within a 2°C range, regardless of the pressure and cooling rate.

Further experimental investigation is required in order to develop realistic probabilistic distributions for nucleation events in industrial systems.

## ACKNOWLEDGEMENTS

The authors thank the financial support received from the CSM Hydrate Consortium of energy companies: BP, Champion, Chevron, ConocoPhillips, ExxonMobil, Halliburton, Petrobras, Schlumberger, Shell, and StatoilHydro and the National Undersea Research Program grant UAF03-0098.

## REFERENCES

- [1] Hammerschmidt E.G. *Formation of Gas Hydrates in Natural Gas Transmission Lines*. Industrial and Engineering Chemistry Research, 1934; 26: 851.
- [2] Turner D. et al. *Development of a Hydrate Kinetic Model and It's Incorporation into the OLGA 2000® Transient Multiphase Flow Simulator*. 5<sup>th</sup> International Conference on Gas Hydrates, 4018, Trondheim, Norway, 2005, p1231-1240.
- [3] Salamantin A.N., Lipenkov V.Y., Ikeda-Fukazawa T. and Hondoh T. *Kinetics of Air-Hydrate Nucleation in Polar Ice Sheets*. Journal of Crystal Growth, 2001; 223: 285-305.
- [4] Salamantin A.N., Hondoh T., Uchida T. and Lipenkov V.Y. *Post-Nucleation Conversion of an Air Bubble to Clathrate Air-Hydrate Crystal in Ice*. Journal of Crystal Growth, 1998; 193: 197-218.
- [5] Ohno H., Lipenkov V.Y. and Hondoh T. *Air Bubble to Clathrate Hydrate Transformation Polar Ice Sheets: A Reconsideration Based on the New Data from Dome Fuji Ice Core*. Geophysical Research Letters, 2004; 31, L21401, doi:10.1029/2004GL021151.
- [6] Shimanda W. and Hondoh T. *In Situ Observation of the Transformation from Air Bubbles to Air Clathrate Hydrate Crystals using a Mizuho Ice Core*. Journal of Crystal Growth, 2004; 265: 309-317.
- [7] Wilson P.W., Lester D. and Haymet A.D.J. *Heterogeneous Nucleation of Clathrates from Supercooled Tetrahydrofuran (THF) / Water Mixtures and the Effect of an Added Catalyst*. Chemical Engineering Science, 2005; 60: 2937-2941.
- [8] Setaram. "Micro DSC VII Commissioning Utilisations." France, Setaram Manual B/DSC7A. 2003.
- [9] Sorai M., ed. *Comprehensive Handbook of Calorimetry and Thermal Analysis*, Wiley 2004
- [10] Lachance, J. *Investigation of Gas Hydrates using Differential Scanning Calorimetry with Water-in-Oil Emulsions*. Colorado School of Mines, Masters Thesis. 2008.